



Title	Generalized modal expansion of electromagnetic field in 2-D bounded and unbounded media
Author(s)	Dai, QI; Chew, WC; Lo, YH; Liu, YG; Jiang, LJ
Citation	IEEE Antennas and Wireless Propagation Letters, 2012, v. 11, p. 1052-1055
Issued Date	2012
URL	http://hdl.handle.net/10722/182785
Rights	IEEE Antennas and Wireless Propagation Letters. Copyright © IEEE

Generalized Modal Expansion of Electromagnetic Field in 2-D Bounded and Unbounded Media

Qi I. Dai, Weng Cho Chew, *Fellow, IEEE*, Yat Hei Lo, Yang G. Liu, and Li Jun Jiang, *Member, IEEE*

Abstract—A generalized modal expansion theory is presented to investigate and illustrate the physics of wave-matter interaction within arbitrary two-dimensional (2-D) bounded and unbounded electromagnetic problems. We start with the bounded case where the field excited by any sources is expanded with a complete set of biorthogonal eigenmodes. In regard to non-Hermitian or non-reciprocal problems, an auxiliary system is constructed to seek for the modal-expansion solution. We arrive at the unbounded case when the boundary tends to infinity or is replaced by the perfectly matched layer (PML). Modes are approximately categorized into two types: trapped modes and radiation modes, which respond differently to environment variations. When coupled with the source, these modes contribute to the modal-expansion solution with different weights, which leads to a reduced modal representation of the excited field in some geometries.

Index Terms—Eigenproblem with perfectly matched layer (PML), generalized modal expansion, reduced modal representation.

I. INTRODUCTION

EIGENMODE expansion (EME) is a powerful tool for the study of many different electromagnetic related applications. At microwave frequencies, efficient analysis of cavity resonators [1] and waveguides [2] by EME are well documented. Moreover, EME is also widely used in modeling a variety of real-life applications in the optical regime [3], including multimode interference (MMI) couplers, photonic crystal fibers, and VCSEL cavities. For example, when a wave guiding structure is investigated, the field is expanded in terms of a complete basis set of local orthogonal eigenmodes of each longitudinal invariant section. Therefore, one can apply mode matching [4] to calculate the field propagation in the whole device. That is, to match the tangential components of modal field at each section interface due to the continuity condition.

Most of the previous literature on EME has a limitation that they are system-specific, mainly on bounded resonating

structures or semi-bounded guiding structures. In this letter, we present a generalized modal-expansion-based analysis that yields a unified treatment of bounded and unbounded electromagnetic problems. To show the idea lucidly without loss of generality, we focus on the 2-D scalar wave problem here. We start with an arbitrary inhomogeneity bounded by a perfect electric conductor (PEC) or a perfect magnetic conductor (PMC). Later, we generalize the analysis to the unbounded case by letting the boundary tend to infinity or replacing the PEC or PMC boundary by the perfectly matched layer (PML). Hence, the same modal expansion process can be applied to the unbounded fields. We include several numerical examples to demonstrate the phenomenon distinguishing trapped modes from radiation modes when the environment varies, and to show a reduced modal representation that may qualitatively approximate the field solution. Our work can provide a different interpretation into the physics of wave interaction with complex structures by using a mode picture of computational electromagnetics (CEM) data. Such physical insight is overlooked by most electromagnetic engineers. Moreover, this work can be extended to 3-D applications. Notice that in this letter, we emphasize on offering physical insight via a modal-expansion-based analysis instead of aiming to develop any fast CEM method.

II. GENERALIZED MODAL EXPANSION THEORY

A. Bounded Case

Consider an arbitrary 2-D ($\partial/\partial z = 0$) linear inhomogeneity in a source-free domain Ω enclosed by a boundary contour Γ . The governing equation for the time-harmonic 2-D scalar wave is written as

$$\left[\nabla \cdot p(\boldsymbol{\rho}) \nabla + \omega^2 \frac{p(\boldsymbol{\rho})}{c^2(\boldsymbol{\rho})} \right] \phi(\boldsymbol{\rho}) = 0 \quad (1)$$

where $\nabla = \hat{x}\partial/\partial x + \hat{y}\partial/\partial y$, $c(\boldsymbol{\rho}) = 1/\sqrt{\epsilon(\boldsymbol{\rho})\mu(\boldsymbol{\rho})}$, and ω^2 are the eigenvalues. For transverse magnetic (TM) waves, $\phi = E_z$ and $p = \mu^{-1}$, while for transverse electric (TE) waves, $\phi = H_z$ and $p = \epsilon^{-1}$. On the boundary Γ , TM waves satisfy $\phi = 0$ when PEC is applied, or $(\partial\phi)/(\partial n) = 0$ when PMC is applied, and TE waves satisfy $\phi = 0$ when PMC is applied, or $(\partial\phi)/(\partial n) = 0$ when PEC is applied. Note that \hat{n} denotes the unit normal vector of contour Γ . The scalar Helmholtz equation given by (1) is essentially a generalized eigenvalue problem in which the eigenmodes ϕ_n of eigenvalues ω_n^2 satisfy

$$\mathcal{L}\phi_n = \omega_n^2 \mathcal{B}\phi_n. \quad (2)$$

Here, $\mathcal{L} = \nabla \cdot p(\boldsymbol{\rho}) \nabla$ and $\mathcal{B} = -p(\boldsymbol{\rho})/c^2(\boldsymbol{\rho})$. The finite extent of domain Ω guarantees the existence of countably infinite eigenmodes for certain discrete values of ω_n^2 . When the bounded medium is Hermitian, or $\epsilon = \epsilon^\dagger$ and $\mu = \mu^\dagger$, both operators \mathcal{L}

Manuscript received June 24, 2012; revised August 18, 2012; accepted August 18, 2012. Date of publication August 27, 2012; date of current version September 27, 2012. This work was supported in part by the Research Grants Council of Hong Kong under Grants GRF 711609 and 711508 and the University Grants Council of Hong Kong under Contract No. AoE/P-04/08.

Q. I. Dai, Y. H. Lo, and L. J. Jiang are with the Department of Electrical and Electronic Engineering, University of Hong Kong, Hong Kong (e-mail: daiqi@hku.hk).

W. C. Chew is with the Department of Electrical and Computer Engineering, University of Illinois at Urbana-Champaign, Urbana, IL 61801 USA, on leave of from the Faculty of Engineering, University of Hong Kong, Hong Kong (e-mail: w-chew@uiuc.edu).

Y. G. Liu is with the Institute of Applied Physics and Computational Mathematics, Beijing 100094, China.

Color versions of one or more of the figures in this letter are available online at <http://ieeexplore.ieee.org>.

Digital Object Identifier 10.1109/LAWP.2012.2215571

and \mathcal{B} can be shown to be Hermitian, based on which we can obtain the orthogonality relations of the eigenmodes as

$$\langle \phi_m, \mathcal{B}\phi_n \rangle = 0, \quad \text{for } \omega_m^2 \neq \omega_n^2 \quad (3)$$

where the inner product is defined to be

$$\langle \psi, \phi \rangle = \int_{\Omega} \psi^*(\boldsymbol{\rho})\phi(\boldsymbol{\rho}) \, d\Omega. \quad (4)$$

Regarding to the degenerate eigenmodes with the same eigenvalues, we can apply the Gram–Schmidt process to orthogonalize them. Equation (1) has no null space for TM wave when PEC boundary is applied and for TE wave when PMC boundary is applied. This is different from the 3-D vector problem where the curl–curl operator has a large null space.

When sources are introduced to domain Ω , the scalar wave equation becomes

$$(\mathcal{L} - \omega^2 \mathcal{B}) \phi(\boldsymbol{\rho}) = S(\boldsymbol{\rho}). \quad (5)$$

Here, the sources S may contain both electric and magnetic currents, i.e.,

$$S = -i\omega J_z + \frac{\partial}{\partial x} (\mu^{-1} M_y) - \frac{\partial}{\partial y} (\mu^{-1} M_x) \quad \text{for TM} \quad (6)$$

$$S = -i\omega M_z - \frac{\partial}{\partial x} (\epsilon^{-1} J_y) + \frac{\partial}{\partial y} (\epsilon^{-1} J_x) \quad \text{for TE.} \quad (7)$$

By using the orthogonality relations in (3), the field solution of (5) can be expanded in terms of the complete set of eigen-basis ϕ_n and their coefficients α_n , given by

$$\phi(\boldsymbol{\rho}) = \sum_{n=1}^{\infty} \alpha_n \phi_n(\boldsymbol{\rho}) = \sum_{n=1}^{\infty} \frac{1}{\omega_n^2 - \omega^2} \frac{\langle \phi_n, S \rangle}{\langle \phi_n, \mathcal{B}\phi_n \rangle} \phi_n(\boldsymbol{\rho}). \quad (8)$$

Note that in the case of lossy (non-Hermitian) but reciprocal medium where $\epsilon = \epsilon^T$ and $\mu = \mu^T$, (8) is still valid provided that the inner product is defined as

$$\langle \psi, \phi \rangle = \int_{\Omega} \psi(\boldsymbol{\rho})\phi(\boldsymbol{\rho}) \, d\Omega. \quad (9)$$

In most cases, the medium may be neither Hermitian nor reciprocal, and hence (3) is no longer valid. More effort needs to be made to seek for a simple expression of α_n . One strategy is to define an auxiliary eigen-problem in the same domain Ω , which may be in the form of [5], [6]

$$\mathcal{L}^T \phi_n^{\text{aux}} = \omega_n^2 \mathcal{B}^T \phi_n^{\text{aux}} \quad (10)$$

where ϕ_n^{aux} satisfy the same boundary condition as ϕ_n in (2). Thus, the orthogonality relations become

$$\langle \phi_m^{\text{aux}}, \mathcal{B}\phi_n \rangle = 0, \quad \text{for } \omega_m^2 \neq \omega_n^2 \quad (11)$$

where the inner product is defined as in (9). Again, degenerate modes can be orthogonalized via the Gram–Schmidt process. Therefore, we can employ (11) to obtain the modal expansion solution of (5) that is

$$\phi(\boldsymbol{\rho}) = \sum_{n=1}^{\infty} \frac{1}{\omega_n^2 - \omega^2} \frac{\langle \phi_n^{\text{aux}}, S \rangle}{\langle \phi_n^{\text{aux}}, \mathcal{B}\phi_n \rangle} \phi_n(\boldsymbol{\rho}). \quad (12)$$

One may also use the periodic boundary condition (PBC) to arrive at a similar expansion formula by following the aforementioned process. However, these eigenmodes become propagating Bloch waves in the PBC case, which is different from the standing modes when bounded by a PEC or PMC.

B. Unbounded Case

The unbounded case is achieved by letting the boundary contour Γ tend to infinity. However, doing this alone may not guarantee the radiation condition. The remedy is to introduce a small loss to Ω , and hence, only outgoing wave solutions are allowed at infinity.

When the boundary is finite, one can approximately divide the global eigenmodes into two types. The first type mainly resonates inside the inhomogeneity such that little energy leaks out. Therefore, they are considered as trapped modes with a high quality factor (high- Q). The rest form the second type, including modes resonating between the inhomogeneity and the boundary, and modes resonating due to the inhomogeneity but efficiently coupling energy to external fields. Such modes should have moderate or low Q values. Note that this categorization is qualitative, however it is useful in many cases due to the physical insight embraced.

As the boundary tends to infinity, the first type of modes remain almost unchanged. They are “immune” to the environment variance, regarding the mode shapes and resonant frequencies. On the other hand, the second type of modes is affected obviously as the boundary expands. They eventually become a continuum from discreteness. Such modes are considered radiation modes since they are able to carry energy to infinity. Now, we can apply the modal expansion analysis to the unbounded problem based on the above approach and approximately rewrite (12) as

$$\phi(\boldsymbol{\rho}) = \sum_{n=1}^N \alpha_n \phi_n(\boldsymbol{\rho}) + \int d\omega' \alpha(\omega') \phi(\omega', \boldsymbol{\rho}) \quad (13)$$

where

$$\alpha_n = \frac{1}{\omega_n^2 - \omega^2} \frac{\langle \phi_n^{\text{aux}}, S \rangle}{\langle \phi_n^{\text{aux}}, \mathcal{B}\phi_n \rangle} \quad (14a)$$

$$\alpha(\omega') = \frac{1}{\omega'^2 - \omega^2} \frac{\langle \phi^{\text{aux}}(\omega'), S \rangle}{\langle \phi^{\text{aux}}(\omega'), \mathcal{B}\phi(\omega') \rangle}. \quad (14b)$$

The first term in (13) corresponds to discrete trapped modes, while the second term corresponds to continuum radiation modes. Strictly speaking, the spectra of both trapped modes and radiation modes broaden when Γ tends to infinity since none of the eigenmodes are completely confined to the inhomogeneity unless the medium has an infinitely high refractive index. Nevertheless, we still keep the trapped modes in a discrete summation form since trapped modes slightly couple with the external environment, resulting in minor spectrum splitting.

In numerical studies, PML of finite extent can be employed to emulate the unbounded case [7]. Stretched-coordinate (SC) PML maps one or more coordinates to complex numbers, resulting in exponentially decaying waves in the PML region rather than oscillating or traveling waves [8]. It has been proven very effective in absorbing outgoing waves. One may apply SC-PML to solve for trapped and radiation modes, which usually play significant roles in modal expansion.

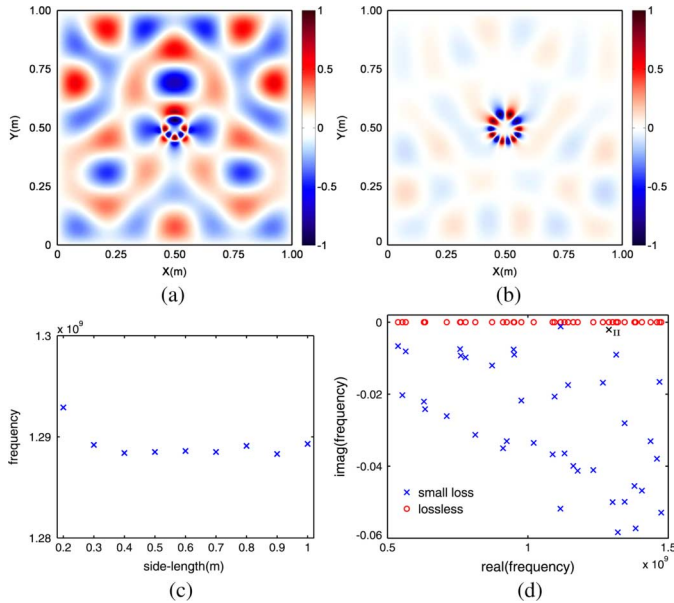


Fig. 1. (a), (b) Field pattern $E_z(x, y)$ (real part) of a radiation mode I and a trapped mode II. (c) Eigenfrequency of mode II when cavity dimension varies. (d) Eigenfrequencies of 40 modes closest to the target frequency 1.1 GHz for both small-loss and lossless case.

III. NUMERICAL SIMULATION STUDY

In this study, the infinite dimensional operator eigenvalue problem (2) is projected onto its subspace and approximated by a finite dimensional matrix eigenvalue problem. There are several ways to discretize (2), such as the finite difference method (FDM), the finite volume method (FVM), and the finite element method (FEM). Here, the Yee-grid-based finite difference method is employed to demonstrate several TM wave ($\phi = E_z$) examples in the frequency domain. To overcome the staircase error, we implement the conformal technique proposed in [9]. The eigensolutions of the resulting sparse eigen-system are solved for by applying the implicitly restarted Arnoldi algorithm [10].

In the first numerical example, an inhomogeneous dielectric ring enclosed by a square PEC cavity is studied to understand how different types of modes behave as we enlarge the cavity dimension. The outer and inner radii of the ring are 0.07 and 0.03 m. The ring is made by two halves, and the relative permittivity of the upper and lower halves are $\epsilon_r^{\text{up}} = 13$ and $\epsilon_r^{\text{low}} = 30$. We place the ring at the center of the cavity whose side length varies from 0.2 to 1 m at a step of 0.1 m. The spatial increment of the Yee grid is chosen to be 1 mm. Fig. 1(a) and (b) show the field pattern $\phi(\rho)$ or $E_z(x, y)$ of a certain radiation (nontrapped) mode I and trapped mode II when the cavity has a dimension of 1×1 m². The real part of the eigenfrequencies between the two eigenmodes are very close, namely 1.2803 and 1.2893 GHz. However, the Q -factor of mode I in Fig. 1(a) is much lower than that of mode II in Fig. 1(b). It is obvious that for the trapped mode, strong resonance occurs inside the inhomogeneity, which confines most of the energy. As the cavity side length increases, the eigenfrequency of mode II varies very slightly as shown in Fig. 1(c), so does its mode shape. On the other hand, radiation modes vary and split as the cavity is made larger, and their spectra become denser and denser, which eventually form a continuum when the boundary tends to infinity. As

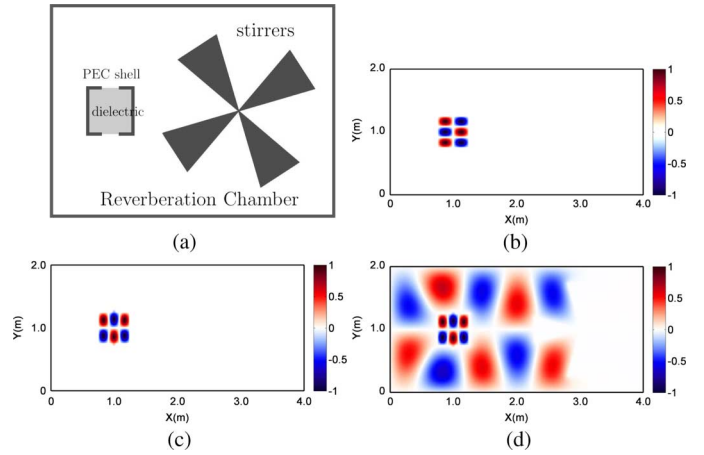


Fig. 2. (a) Simulation geometry. (b) $E_z(x, y)$ of mode TM_{23} at stirrer's angle $(\pi)/3$. (c), (d) $E_z(x, y)$ of mode TM_{32} at stirrer's angle $(\pi)/3$ and 0.

mentioned above, a small loss is introduced to the cavity such that we assume the imaginary part of the free-space permittivity to be 10^{-10} . Therefore, the eigenfrequencies become complex. The trapped modes can be easily identified since their eigenfrequencies have a relatively small imaginary part. Eigenfrequencies of 40 modes closest to the target frequency 1.1 GHz for both small-loss and lossless cases are illustrated in Fig. 1(d). For the small-loss case, the eigenfrequency with the second smallest imaginary part (in magnitude) corresponds to mode II as shown in Fig. 1(b).

In the second example, we further demonstrate how trapped modes respond to the variance of the environment. In a 2-D TM reverberation chamber, a dielectric of relative permittivity $\epsilon_r = 12$ bounded by a PEC shell couples with the externality through two small apertures [Fig. 2(a)]. The stirrers are made by metals of high conductivity. The dimensions of the chamber and the dielectric are 4×2 and 0.5×0.5 m². The FD grid length is taken to be 0.0125 m. We seek for trapped modes of eigenfrequencies closest to 300 MHz. Fig. 2(b) displays a trapped mode TM_{23} corresponding to an unchanged eigenvalue 3.1138×10^8 (real part). Due to the position of the apertures, mode TM_{32} has a lower Q -factor than TM_{23} , but we still consider it to be trapped [Fig. 2(c)] since its mode shape and eigenfrequency remain almost unchanged when the stirrer's angle changes. Fig. 2(d) shows the field pattern when the trapped mode TM_{32} couples with the external mode at a certain stirrer's angle. On the other hand, trapped mode TM_{23} does not couple to the external mode regardless of the stirrer's angle due to its higher Q -factor.

In the third example, we present the reduced modal representation of an unbounded field based on modal expansion. The geometry under study is illustrated in Fig. 3(a) where a cavity with an aperture is partially filled by a dielectric. The walls of the cavity are modeled as PEC, and the relative permittivity of the dielectric ϵ_r is 2.2. The overall computational domain occupies 100×100 Yee grids. The size of each Yee grid is taken as 0.01×0.01 m². The cavity has a dimension of 0.2×0.16 m², while the dielectric has a dimension of 0.05×0.16 m². The aperture is only 0.03 m wide. A 10-layer PML is added to each wall of the domain to effectively reduce the artificial reflection. A z -polarized current source is placed as shown in Fig. 3(a)

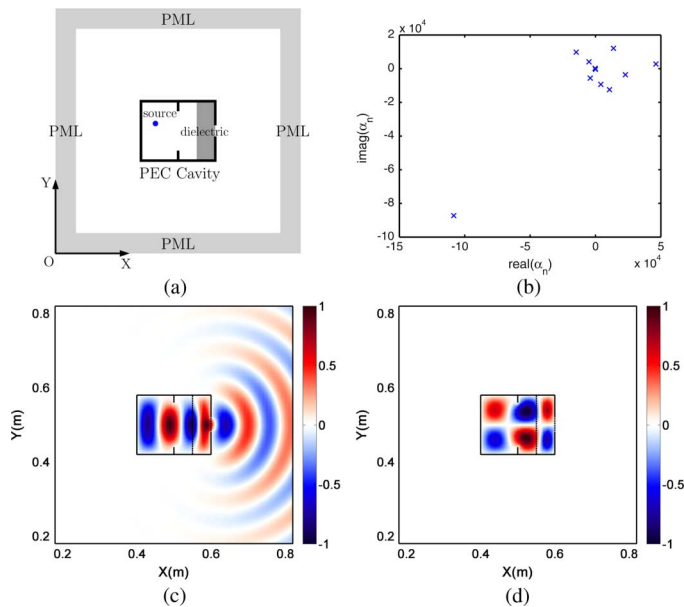


Fig. 3. (a) Simulation geometry. (b) Weighting coefficients of expansion eigenmodes. (c), (d) Imaginary parts of field distribution for eigenmodes with the largest and second largest weighting coefficient.

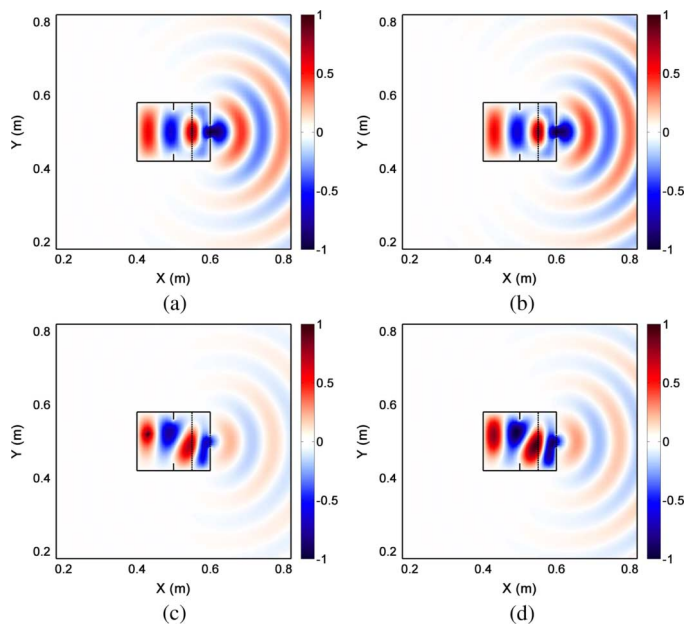


Fig. 4. (a) Real part of $E_z(x, y)$ by direct solution. (b) Real part of $E_z(x, y)$ by modal expansion. (c) Imaginary part of $E_z(x, y)$ by direct solution. (d) Imaginary part of $E_z(x, y)$ by modal expansion.

to generate a TM field. The working frequency is chosen to be 2.7 GHz. In the simulation geometry, the point source excites several eigenmodes and couples energy to each of them with different complex weights, which are determined by (13) and plotted as in Fig. 3(b). Most of the source energy is taken by the eigenmode with the largest weighting coefficient $\alpha_n = (-10.838 - 8.7259i) \times 10^4$ [Fig. 3(c)], which not only resonates due to the cavity confinement, but also carries the source

energy out of the cavity to infinity through the aperture. A different case is the eigenmode with the second largest coefficient $\alpha_n = (4.6226 + 0.27548i) \times 10^4$ [Fig. 3(d)], which only resonates within the cavity, with little modal energy leaking out. Such a trapped mode can be identified from the eigenfrequencies of very small imaginary parts, since the imaginary part of the eigenfrequency indicates damping. Large damping is a result of energy dissipation that corresponds to radiation in this example. The field solution under the source excitation, on one hand, can be obtained by directly solving the discretized matrix equation resulted from (5). Fig. 4(a) and (c) shows the real and imaginary part of the field response $E_z(x, y)$, respectively. On the other hand, the solution may be approximated by the weighted sum of several significant modes. Here, we take advantage of 11 most crucial eigenmodes to obtain the modal-expansion solution, the real and imaginary part of which are shown in Fig. 4(b) and (d), respectively. By comparison, we find that the modal-expansion solution is a reasonably good approximation of the original field solution, which indicates that only a few significant modes are needed to qualitatively represent the field distribution in this example.

IV. CONCLUSION

A generalized modal expansion theory of a 2-D electromagnetic field in both bounded and unbounded media has been proposed. A reduced modal representation of the field response under excitation has been presented. Excited fields can be represented approximately by a small number of trapped and radiation modes. This work applies CEM techniques to assist the modal analysis. It also offers useful physical insight in the microwave device and antenna design.

REFERENCES

- [1] R. E. Collin, *Field Theory of Guided Waves*. New York: IEEE Press, 1991.
- [2] A. Hardy and M. Ben-Artzi, "Expansion of an arbitrary field in terms of waveguide modes," *Inst. Elect. Eng. Proc., Optoelectron.*, vol. 141, no. 1, pp. 16–20, 1994.
- [3] N. Issa and L. Poladian, "Vector wave expansion method for leaky modes of microstructured optical fibers," *J. Lightw. Technol.*, vol. 21, no. 4, pp. 1005–1012, Apr. 2003.
- [4] D. Arena, M. Ludovico, G. Manara, and A. Monorchio, "Analysis of waveguide discontinuities using edge elements in a hybrid mode matching/finite elements approach," *IEEE Microw. Wireless Compon. Lett.*, vol. 11, no. 9, pp. 379–381, Sep. 2001.
- [5] C. H. Chen and C.-D. Lien, "The variational principle for non-self-adjoint electromagnetic problems," *IEEE Trans. Microw. Theory Tech.*, vol. MTT-28, no. 8, pp. 878–886, Aug. 1980.
- [6] W. C. Chew, *Waves and Fields in Inhomogeneous Media*. Piscataway, NJ: IEEE Press, 1995.
- [7] J. P. Berenger, "A perfectly matched layer for the absorption of electromagnetic waves," *J. Comput. Phys.*, vol. 114, pp. 185–200, 1994.
- [8] W. C. Chew and W. H. Weedon, "A 3D perfectly matched medium from modified Maxwell's equations with stretched coordinates," *Microw. Opt. Technol. Lett.*, vol. 7, pp. 599–604, 1994.
- [9] W. Yu and R. Mittra, "A conformal finite difference time domain technique for modeling curved dielectric surfaces," *IEEE Microw. Wireless Compon. Lett.*, vol. 11, no. 1, pp. 25–27, Jan. 2001.
- [10] R. Lehoucq and D. Sorensen, "Deflation techniques for an implicitly restarted Arnoldi method," *SIAM J. Matrix Anal. Appl.*, vol. 17, no. 4, pp. 789–821, 1996.